RSC Advances

PAPER

Check for updates

In situ-DRIFTS study: influence of surface acidity of rhenium-based catalysts in the metathesis of various olefins for propylene production

Siriporn Vorakitkanvasin,[a] Weena Phongsawat,[b] Kongkiat Suriye,[b] Piyasan Praserthdam[a] and Joongjai Panpranot (ID) *[a]

Various olefins including 1- and 2-butene, 2-pentene, and ethylene were used as the reactants for producing propylene by self- and cross-metathesis reactions at 60 °C on supported Re-based catalysts (4 wt% Re). A similar surface structure of rhenium oxides in the form of isolated ReO_4 species was observed on Al_2O_3 and SiO_2–Al_2O_3 supported rhenium oxide catalysts. The catalysts, however, differed in terms of the types (Lewis/Bronsted) and strengths of the acidic sites, as revealed by ammonia temperature programmed desorption (NH_3-TPD) and *in situ* diffuse reflectance infrared Fourier transform spectroscopy (*in situ* DRIFTS) of NH_3 adsorption and thermodesorption results. Weak Lewis acidity, especially high ratios of Lewis acid bands at 1280 cm^{-1}/1622 cm^{-1}, led to high metathesis activity of the Re-based catalysts. The additional isomerization activity, however, required strong Bronsted acid sites. The product distribution from the various feeds depended largely on the size of the olefins, and not only on the acid properties of the catalysts. Re_2O_7/SiO_2–Al_2O_3 appeared to be a versatile catalyst for obtaining a high yield of propylene using either a single reactant (1- or 2-butene) or an ethylene mixed feed.

1. Introduction

Propylene is one of the major feedstocks in the petrochemical industry used to produce various chemical intermediates and polymers. Since propylene demand is expected to continue to grow, on-purpose propylene production technology, such as olefin metathesis, is becoming an increasingly important reaction for propylene supply.[1] Metathesis of ethylene and 2-butene to propylene is typically carried out over heterogeneous catalysts based on tungsten oxide, molybdenum oxide, and rhenium oxide.[2–4] Rhenium oxide-based catalysts are of interest because of their high activity and selectivity for olefin metathesis at low reaction temperatures.[3] The typical supports used for preparation of highly dispersed rhenium oxide catalysts are alumina and silica-alumina.[3,5–7]

Surface structures of the active isolated ReO_4 species on alumina have been identified by a number of studies based on Raman, *in situ* Raman, and *in situ* IR spectroscopy.[8–13] The surface rhenium oxide species presented on silica-alumina support were similar to those of alumina supported ones but they were inactive on the Si–OH.[14] Besides, the catalytic performances of supported rhenium oxide-based catalysts have

often been correlated to either Bronsted[15] or Lewis acid sites.[16] Bouchmella *et al.*[17] used a nonhydrolytic sol–gel method (NHSG) to prepare highly active Re–Si–Al metathesis catalysts. The most active NHSG catalyst in the cross-metathesis of ethylene and butene to propylene was found on the catalysts containing the highest amount of acidic sites with well dispersed rhenium oxide species and high surface areas. A recent study from our group[11] showed that the higher acidic OH group on the alumina support provided higher Lewis acid sites necessary for the formation of the rhenium oxide active species whereas the higher Bronsted acidity led to higher amount of coke and C_{5+} products. In addition, the acid strength of Lewis acid sites appeared to be another important factor determining metathesis activity of supported Re_2O_7 catalysts.

Due to olefins price fluctuation, nowadays ethylene price is getting higher than propylene,[18] therefore, other reactants such as butene and pentene are considered as alternative reactants for metathesis reaction for propylene production. This work aims to define the catalyst properties especially the types (Lewis or Bronsted) and the strength of the acidic sites on supported rhenium oxide-based catalysts that could provide high yield of propylene from different feedstocks. Production of propylene *via* the metathesis of ethylene and 2-butene, ethylene and 2-pentene, pure 2-butene, pure 1-butene, and pure 2-pentene was obtained over the low rhenium loading catalysts (4 wt% Re) supported on silica and silica-alumina. The surface structures of rhenium oxide species were determined by Raman microscopy. The types and the strength of acidity on the catalyst

[a] *Center of Excellence on Catalysis and Catalytic Reaction Engineering, Department of Chemical Engineering, Faculty of Engineering, Chulalongkorn University, Bangkok 10330, Thailand. E-mail: joongjai.p@chula.ac.th; Fax: +66-2218-6877; Tel: +66-2218-6869*

[b] *SCG Chemicals Co., Ltd, 1Siam-cement Rd, Bang sue, Bangkok 10800, Thailand*

surface were identified by ammonia temperature programmed desorption (NH₃-TPD) and *in situ* diffuse reflectance infrared Fourier transform spectroscopy (*in situ* DRIFTS) of NH₃ adsorption and thermodesorption.

2. Experimental

2.1 Catalyst preparation

Supported rhenium oxide catalysts with 4 wt% rhenium loading were prepared by the incipient wetness impregnation method using an aqueous solution of ammonium perrhenate (NH₄ReO₄, Aldrich). The supports were impregnated several times to obtain the 4 wt% of rhenium loading. Between impregnation steps, the catalysts were held for 2 h at room temperature and then dried at 110 °C for 12 h. After the impregnation step, the catalysts were calcined in dry air at 550 °C for 8 h. For comparison purposes, commercial γ-Al₂O₃ (Fluka) and SiO₂–Al₂O₃ (Grade 135, Aldrich) were employed as the support for the preparation of Re₂O₇/γ-Al₂O₃ and Re₂O₇/SiO₂–Al₂O₃ catalysts. The catalysts were denoted as Re/Al and Re/SiO₂–Al₂O₃, respectively. The ANN support was prepared by calcination of aluminium nitrate (Al(NO₃)₃·9H₂O) under air at 550 °C for 4 h. The rhenium catalyst on ANN was denoted as Re/ANN. According our previous paper, the use of alumina support prepared from ANN calcined at 550 °C led to the formation of higher amount of the second rhenium oxide species and improved catalytic performances in the metathesis of ethylene and 2-pentene than the conventional Re₂O₇/γ-Al₂O₃.[11]

2.2 Catalyst characterization

The surface structures of rhenium oxide species were examined by Raman microscopy under ambient conditions using a Senterra Dispersive Raman microscopy equipped with the visible laser at 532 nm and a TE-cooled CCD detector. The amount of acidity on catalyst surface was measured by the NH₃-TPD in a quartz U-tube reactor. Firstly, approximately 0.10 g catalyst sample was pretreated in a helium gas flow (25 mL min⁻¹) at 500 °C for 1 h and then cooled down to 40 °C. After that, the sample was saturated with 15% NH₃/He. The physisorbed ammonia was desorbed in a helium gas flow for about 2 h. Finally, the sample was heated up from 40 to 500 °C at a heating rate 10 °C min⁻¹. The amount of ammonia in effluent was recorded *via* TCD signal and analyzed with a Micromeritic Chemisorb 2750 automated system (ChemiSoftTPx software). The *in situ* diffuse reflectance infrared Fourier transform spectroscopy (DRIFTS) of NH₃ adsorption spectra were recorded with a Bruker Vertex-70 FT-IR spectrometer equipped with a Harrick Praying Mantis attachment for diffuse reflectance spectroscopy. About 20–25 mg of sample was placed in a Harrick cell, which were cooled by flowing water. Then, the sample was dehydrated at a heating rate of 10 °C min⁻¹ up to 500 °C and held for 1 h in a nitrogen gas flow. After that, the sample was cooled to 60 °C. After pretreatment procedure, the sample was saturated with 15% NH₃/He. After saturation, the physisorbed ammonia was desorbed in a nitrogen gas flow about 2 h. Then, the sample was heated from 60 °C temperature to 500 °C

at a heating rate 10 °C min⁻¹. The spectra were collected using a MCT detector with a resolution of 4 cm⁻¹ and an accumulation of 64 scans.

2.3 Reaction test

The performances of supported rhenium oxide catalysts were evaluated in the metathesis reactions using 2-pentene and ethylene (2-C₅ + C₂), pure 2-pentene (2-C₅), 2-butene and ethylene (2-C₄ + C₂), pure 2-butene (2-C₄) and pure 1-butene (1-C₄) as the reactants. For the cross metathesis reaction (mixed feeds), an excess of the molar ratio of ethylene : 2-pentene and ethylene : 2-butene was used for the reaction tests. The reactants were mixed with high purity nitrogen in order to have the composition of 6 vol% of reactants in nitrogen balance. The reactions were carried out with a weight hourly space velocity (WHSV) 1.7 h⁻¹ using 1.5 g catalyst in a fixed-bed reactor (ID tube = 15.8 mm) under atmospheric pressure. Prior to the reaction, the catalyst was pretreated at 500 °C for 1 h and then cooled down to reaction temperature 60 °C under nitrogen flow. During the reaction, both reactants and products were analyzed by an on-line Agilent 7820A gas chromatograph equipped with a GS-Gaspro 113-4362 capillary column, 0.32 mm diameter and 60 m in length. The GC signals were processed by an EZChrom Elite integrated peak program integrator.

3. Results and discussion

3.1 Catalyst characterization

The low loading Re oxide catalysts (4 wt% Re) in this study were prepared on three different supports including commercial γ-alumina (Re/Al), alumina obtained by calcination of aluminium nitrate at 550 °C (Re/ANN), and commercial silica-alumina (Re/SiO₂–Al₂O₃). All the catalysts exhibited similar Raman bands at 970, 920 and 325 cm⁻¹ under ambient conditions, which were assigned to ν_s(Re=O), ν_{as}(Re=O), and
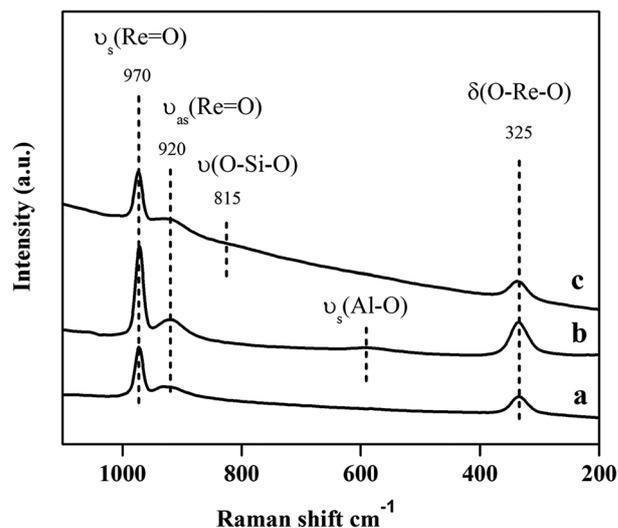

Fig. 1 The Raman spectra of: (a) Re/Al, (b) Re/ANN and (c) Re/SiO₂–Al₂O₃ under ambient condition.

$\delta_{a,as}$(O–Re–O), respectively (Fig. 1). Such results indicate that the surface rhenium oxide species on the prepared catalysts were presented in the form of isolated ReO$_4$ structure. Additional strong Raman band at 815 cm^{-1} of the Re/SiO$_2$–Al$_2$O$_3$ was due to the interference from the SiO$_2$.[8] A small band at around 600 cm^{-1} was detected for the Re/ANN catalyst and was assigned to the Al^{3+}–oxygen symmetric stretching mode of the [Al(OH$_2$)$_6$]$^{3+}$ cation, which was resulted from the decomposition of Al(NO$_3$)$_3$·9H$_2$O precursor.[19,20]

The Re/Al, Re/ANN, and Re/SiO$_2$–Al$_2$O$_3$ differed largely on the nature of acidity (total amount, acid strength, and type of acidity). As shown by the NH$_3$-TPD profiles in Fig. 2, the areas under the NH$_3$-TPD profiles were in the order: Re/SiO$_2$–Al$_2$O$_3$ > Re/ANN > Re/Al. The Re/Al and the Re/ANN exhibited only weak and medium acidity whereas the Re/SiO$_2$–Al$_2$O$_3$ exhibited weak, medium, and strong acidity. The peak area for weak acidity of the Re/ANN was slightly higher than that of the Re/Al. The types of surface acidity on these catalysts were elucidated by the *in situ* DRIFTS of adsorbed NH$_3$ and the results are shown in Fig. 3. The bands at 1280 and 1622 cm^{-1} assigned to adsorbed NH$_3$ on Lewis acid sites and the bands at 1470 and 1686 cm^{-1} assigned to NH$_4^+$ on Bronsted acid sites were detected for all the rhenium oxide catalysts.[11,21–23] Additional broad bands at 1240, 1405, 1506, 1570 cm^{-1} were assigned to NH$_2$ vibration.[23–25] The amounts of Bronsted and Lewis acid sites calculated from the integrated peak areas based on the *in situ* DRIFTS results are given in Table 1. The areas of Lewis acid sites at 1280 cm^{-1} were in the order: Re/SiO$_2$–Al$_2$O$_3$ > Re/ANN > Re/Al whereas and opposite trend was found for another Lewis acid sites at 1622 cm^{-1}. The area for the Bronsted acid sites at 1470 cm^{-1} of the Re/SiO$_2$–Al$_2$O$_3$ catalyst was much larger than the Re/ANN and Re/Al catalysts. Such results suggest that additional strong acidity observed in the NH$_3$-TPD profiles for the Re/SiO$_2$–Al$_2$O$_3$ were strong Bronsted acid sites.

The relative strength of Bronsted and Lewis acid sites present on the different catalysts was compared by the *in situ* DRIFTS of thermodesorption of NH$_3$ experiments (Fig. 4). It was found that the bands corresponding to the Bronsted acid sites on Re/ANN and Re/Al markedly decreased with increasing temperature starting from 100 °C whereas those of Re/SiO$_2$–

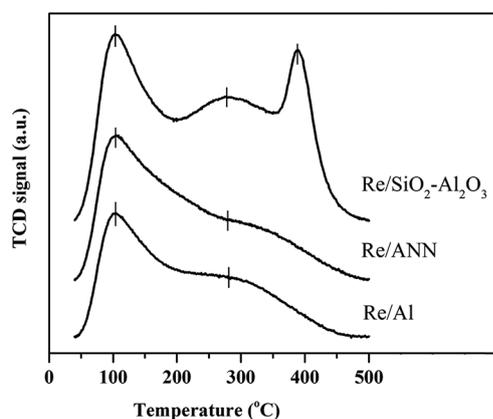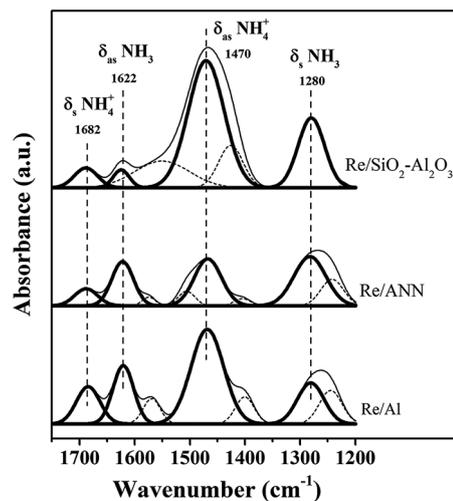Fig. 3 The *in situ* DRIFTS substracted spectra of the chemisorbed ammonia over the catalysts at 60 °C.

Al$_2$O$_3$ started to decrease after the temperature was raised to above 250 °C. In the present work, the fractions of weak and strong Bronsted and Lewis acid sites were calculated from subtracted peak areas of the *in situ* DRIFTS of NH$_3$ thermodesorption results as summarized in Table 2. The peak areas in the temperature range lower and above 250 °C were assigned to weak and strong acid sites, respectively. The fractions of weak and strong Lewis acid sites on all the catalysts were not significantly different. The fraction of Bronsted acid sites on the Re/ANN and Re/Al catalysts inclined to the weak acid while most of the Bronsted acid sites on the Re/SiO$_2$–Al$_2$O$_3$ catalyst was classified as strong acid.

3.2 Reaction results

The supported rhenium oxide catalysts with different acid properties were employed in the metathesis reaction using various reactants including 2-pentene and ethylene (2-C$_5$ + C$_2$), pure 2-pentene (2-C$_5$), 2-butene and ethylene (2-C$_4$ + C$_2$), pure 2-butene (2-C$_4$), and pure 1-butene (1-C$_4$) at 60 °C, 1 atm, and WHSV 1.7 h^{-1}. The yield of propylene of the catalysts with various feedstocks after 8 h reaction time are shown in Fig. 5. From the results, it was found that for a given set of reactants, the SiO$_2$–Al$_2$O$_3$ supported Re$_2$O$_7$ catalysts gave much higher yield of propylene than the Al$_2$O$_3$ supported ones. The yields of propylene obtained from the Re/SiO$_2$–Al$_2$O$_3$ were in order: 2-C$_4$ + C$_2$ > 2-C$_5$ + C$_2$ > 1-C$_4$ > 2-C$_4$ > 2-C$_5$. On the other hand, the Re/ANN and Re/Al produced the highest propylene yield when 2-C$_5$ and C$_2$ were used as the reactants under the reaction conditions used with the Re/ANN exhibited higher propylene yield than the Re/Al. The distribution of products obtained from various feedstocks over the Re/SiO$_2$–Al$_2$O$_3$, Re/ANN, and Re/Al are shown in Fig. 6. The major reactions involved in the propylene production from various feedstocks are shown below in eqn (1) to (9).
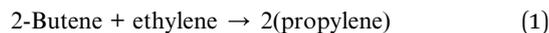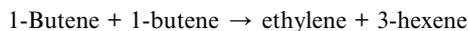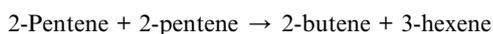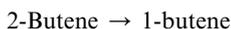
Primary metathesis reactions

Fig. 2 NH$_3$-TPD profiles of different catalysts.

$$2\text{-Butene} + \text{ethylene} \rightarrow 2(\text{propylene}) \qquad (1)$$

Table 1 The amounts of Bronsted and Lewis acid sites over the catalysts determined from the *in situ* DRIFTS of adsorbed NH_3 at 60 °C after pretreatment
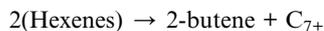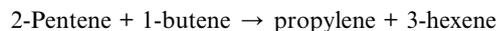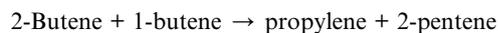
Catalyst	Bronsted acid (a.u.) (1682 cm^{-1})	Lewis acid (a.u.) (1622 cm^{-1})	Bronsted acid (a.u.) (1470 cm^{-1})	Lewis acid (a.u.) (1280 cm^{-1})	Lewis acid (1280 cm^{-1})/(1622 cm^{-1})
Re/SiO$_2$–Al$_2$O$_3$	3.5	2.2	35.4	14.2	6.4
Re/ANN	3.0	7.4	10.9	12.1	1.6
Re/Al	6.7	9.3	21.9	8.4	0.9

$$\text{2-Pentene + ethylene} \rightarrow \text{propylene + 1-butene} \quad (2)$$

$$\text{2-Pentene + 2-pentene} \rightarrow \text{2-butene + 3-hexene} \quad (3)$$

$$\text{1-Butene + 1-butene} \rightarrow \text{ethylene + 3-hexene} \quad (4)$$

Isomerization reaction

$$\text{1-Butene} \rightarrow \text{2-butene} \quad (5)$$

$$\text{2-Butene} \rightarrow \text{1-butene} \quad (6)$$

Secondary metathesis reactions

$$\text{2-Butene + 1-butene} \rightarrow \text{propylene + 2-pentene} \quad (7)$$

$$\text{2-Pentene + 1-butene} \rightarrow \text{propylene + 3-hexene} \quad (8)$$

$$\text{2(Hexenes)} \rightarrow \text{2-butene + C}_{7+} \quad (9)$$

According to the stoichiometry of reaction, the mixed ethylene and 2-butene provides the highest yield of propylene. Using this feed, the Re/SiO$_2$–Al$_2$O$_3$ exhibited high metathesis activity for the cross-metathesis of ethylene and 2-butene (eqn (1)), producing propylene as the major product with very low amount of isomerization side reaction products. Surprisingly, little propylene was produced when using the mixed ethylene and 2-butene feedstocks on the Re/ANN and the Re/Al catalysts. It is likely that only the self metathesis of 2-butene occurred on the alumina-supported rhenium oxide catalysts under the reaction conditions used.

Using mixed ethylene and 2-pentene as the feedstocks, the major product selectivity obtained on the Re/SiO$_2$–Al$_2$O$_3$ were propylene and 2-butene with 1-butene, hexenes, and C$_{7+}$ as the minor products. On the contrary, on the Re/Al and the Re/ANN, 2-butene and hexenes were the main products with lower selectivity to propylene and 1-butene. From the product distribution results, it reveals that both cross metathesis of ethylene
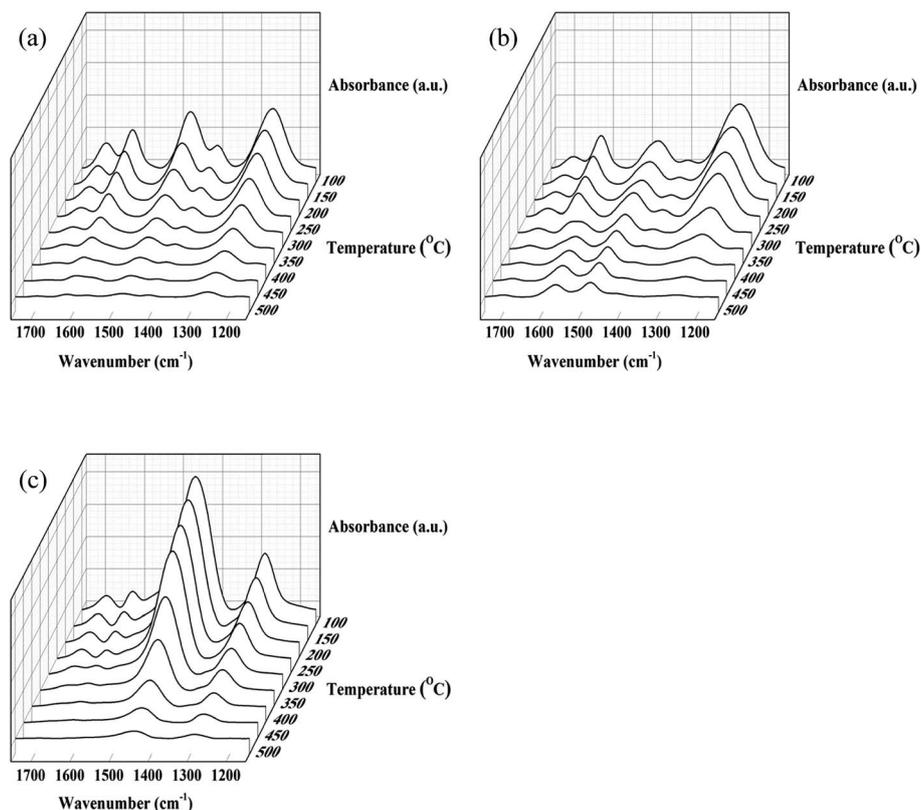

Fig. 4 The *in situ* DRIFTS of NH_3 adsorption spectra with increment of temperature: (a) Re/Al, (b) Re/ANN and (c) Re/SiO$_2$–Al$_2$O$_3$.

Table 2 The fraction of strength of the Bronsted and Lewis acid sites determined from the *in situ* DRIFTS of NH_3 thermodesorption

Catalyst	BA (1682 cm^{-1})		LA (1622 cm^{-1})		BA (1470 cm^{-1})		LA (1280 cm^{-1})	
	Weak	Strong	Weak	Strong	Weak	Strong	Weak	Strong
Re/SiO$_2$–Al$_2$O$_3$	62	38	76	24	32	68	54	46
Re/ANN	49	51	47	53	61	39	55	45
Re/Al	79	21	63	37	82	18	55	45

and 2-pentene (eqn (2)) and self-metathesis of 2-pentene (eqn (3)) occurred on all the catalysts. However, as suggested by Lwin *et al.*,[13] the rate-determining step of metathesis reaction is the rate of olefin adsorption and the adsorption rate increases with the size of olefins (*i.e.*, $C_4^= > C_3^= > C_2^=$). Thus, the self-metathesis of 2-pentene may occur more easily than the cross-metathesis of ethylene and 2-pentene. In addition, due to the higher isomerization activity of the Re/SiO$_2$–Al$_2$O$_3$, 1-butene, which was one of the products from the cross-metathesis of ethylene and 2-pentene, was isomerized to 2-butene (eqn (5)) and further reacted with excess ethylene to produce augmentative propylene.

Using 2-butene as the single feedstock, the Re/Al and Re/ANN were not active under the conditions used while the Re/SiO$_2$–Al$_2$O$_3$ produced propylene and 2-pentene as the main products. It is indicated that 2-butene was isomerized to 1-butene (eqn (6)) and then reacted with 2-butene to produce propylene and 2-pentene according to eqn (7) and (8). In the case of using 1-butene as the single feedstock, the Re/Al and Re/ANN were active for the self-metathesis of 1-butene, forming ethylene and 3-hexene products (eqn (4)). Since propylene and 2-pentene were also observed, it is suggested that isomerization of 1-butene to 2-butene (eqn (5)) occurred on these catalysts and then further underwent the secondary metathesis reaction between 1-butene and 2-butene (eqn (7)). It should be noted that these catalysts were active enough to isomerization 1-butene to 2-butene but they could not isomerize 2-butene to 1-butene. From the product distribution results, the Re/SiO$_2$–Al$_2$O$_3$ appeared to be much more active than the Al$_2$O$_3$ supported ones. Additional propylene production was obtained from the

cross metathesis of ethylene and 2-butene on the Re/SiO$_2$–Al$_2$O$_3$ (eqn (1)). Although propylene could not be obtained using 2-pentene as the single reactant, the catalysts were active enough to catalyze 2-pentene self-metathesis reaction, yielding 2-butene and 3-hexene (eqn (3)). And due to their much higher activity, the Re/SiO$_2$–Al$_2$O$_3$ exhibited additional side reactions self-metathesis of hexene, forming C$_{7+}$ products (eqn (9)).

In summary, in order to produce propylene using pure feedstocks such as 1-butene and 2-butene, the catalyst must exhibit high isomerization activity to convert 1-butene to 2-butene and 2-butene to 1-butene in addition to high metathesis activity. Under the reaction conditions used, the isomerization of 1-butene to 2-butene occurred more easily than the isomerization of 2-butene to 1-butene.

3.3 Activity–acidity relationship

Due to the interference of the SiO$_2$ bands in the Raman spectra, it was difficult to quantitatively determine the amount of active Re species on the Re/SiO$_2$–Al$_2$O$_3$ in order to compare with the Al$_2$O$_3$ supported ones. The catalyst performances in this study, thus, were correlated to the acidity presented. Nevertheless, it should be noted that acidity was arisen from both the rhenium oxide species and the supports themselves. Based on the NH$_3$-IR results of the catalysts at 60 °C after pretreatment (Table 1), which represented the surface species before reaction, it was found that the Re/Al catalysts possessed significant amount of Bronsted acidity but they exhibited the lowest activity for both isomerization and metathesis reactions. It is suggested that the strength of acidity should be taken into account as well. From the calculated fractions of weak and strong Bronsted and Lewis acid sites based on the *in situ* DRIFTS of NH$_3$ adsorption and thermodesorption results, only the Re/SiO$_2$–Al$_2$O$_3$ displayed emphatically strong Bronsted acidity. The Re/Al contained relatively high quantity of Bronsted acidity but most of them was weak acid. From these results, it is suggested that the strong Bronsted acidity was necessary for the isomerization of 2-butene to 1-butene. On the other hand, there were no differences in terms of the fractions of weak and strong Lewis acid among the prepared catalysts. A number of studies in the literature suggested that Lewis acidity plays significant role in metathesis reaction.[11,21] The present work, however, revealed various Lewis acid sites with different bond strengths on the supported Re oxide catalysts. It was found that the higher ratios of the weak Lewis acid bands at wavenumber 1280 cm^{-1}/1622 cm^{-1} led to higher metathesis activity as observed in the order: Re/SiO$_2$–Al$_2$O$_3$ ≫ Re/ANN > Re/Al. From the reaction test results, the Re/SiO$_2$–Al$_2$O$_3$ showed high activity in all the
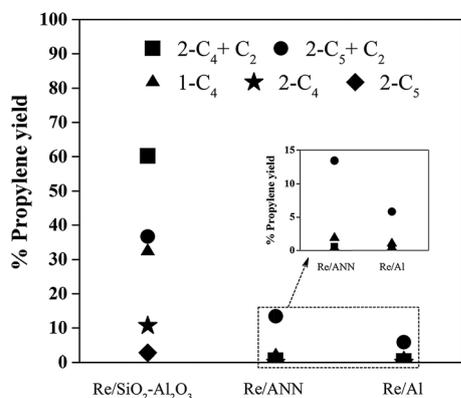
Fig. 5 The yield of propylene of the catalysts with various feedstocks at 8 h reaction time.
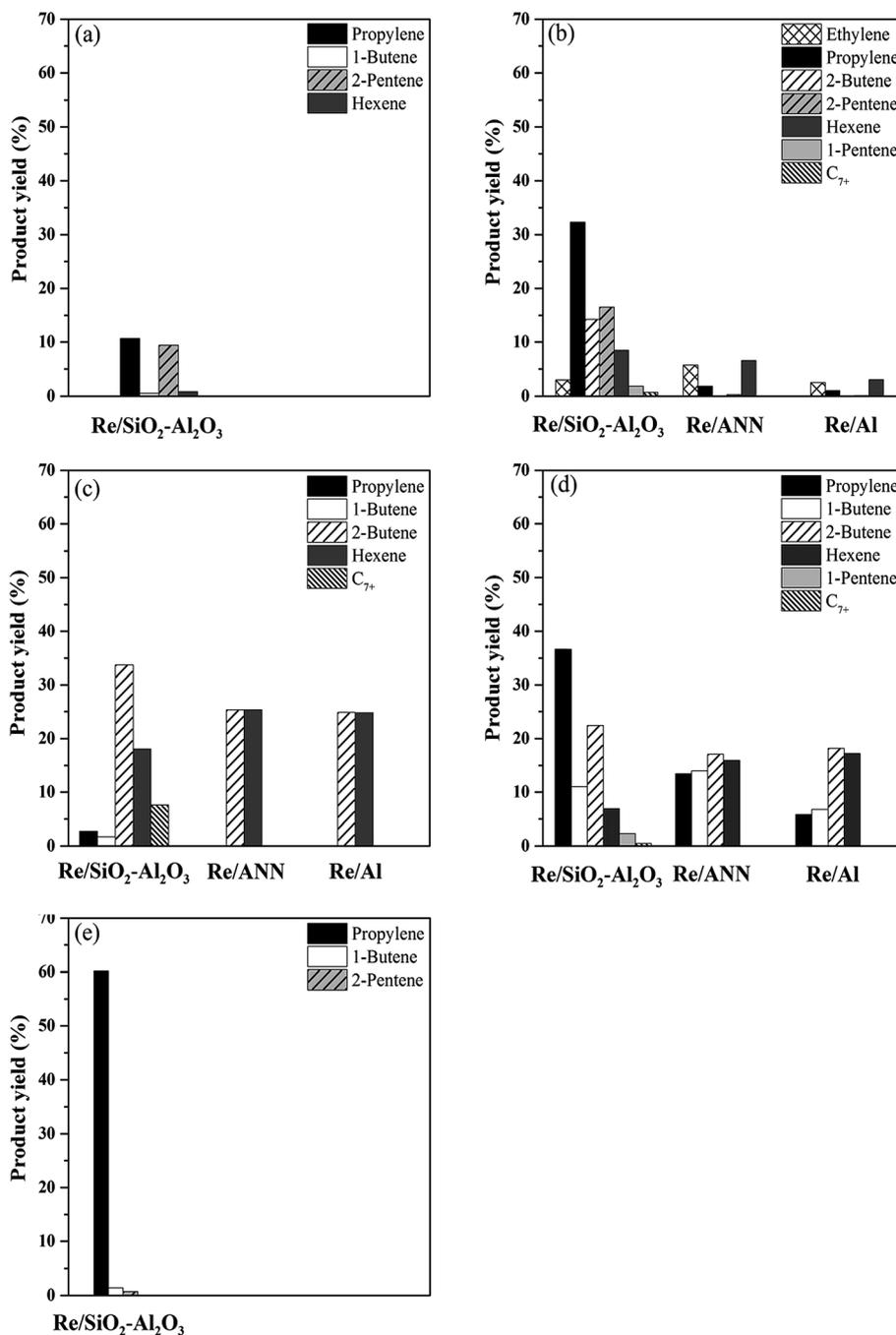
Fig. 6 Product distributions of various feedstocks over the catalysts: (a) pure 2-butene, (b) pure 1-butene, (c) pure 2-pentene, (d) mixed ethylene and 2-pentene and (e) mixed ethylene and 2-butene.

reactions necessary for propylene production from various feedstocks including isomerization of 2-butene to 1-butene and self- and cross-metathesis reactions, resulting in the highest yield of propylene. Therefore, to handle ethylene–propylene price fluctuation, supported rhenium oxide-based catalysts should possess certain weak Lewis acid species (high ratio of weak Lewis acid bands at wavenumber 1280 cm^{-1}/1622 cm^{-1}) and strong Bronsted acid sites. Generally, the role of SiO$_2$ in SiO$_2$–Al$_2$O$_3$ supported rhenium

oxide catalysts has been related to the bridging of the silanol groups (Si–OH) with the Al$_2$O$_3$ in the form of Si–OH–Al. These bridging hydroxyl groups generate active rhenium sites while silanol groups would generate inactive rhenium sites.[3,5,26] The high olefins metathesis activity of SiO$_2$–Al$_2$O$_3$ supported rhenium oxides thus could not be generalized for any SiO$_2$–Al$_2$O$_3$ support since it was found to depend on many factors such as the SiO$_2$–Al$_2$O$_3$ composition[27] and the preparation method of SiO$_2$–Al$_2$O$_3$.[17,28]

4. Conclusions

The low loading Re/SiO$_2$–Al$_2$O$_3$ catalyst allows the production of propylene from various feedstocks. Under the reaction conditions used (60 °C, 1 atm), the yield of propylene from different feeds was in the order: 2-C$_4$ + C$_2$ > 2-C$_5$ + C$_2$ > 1-C$_4$ > 2-C$_4$ > 2-C$_5$. The high metathesis activity was correlated well to the presence of high ratio of the Lewis acidity bands (1280 cm^{-1}/1622 cm^{-1}) in the form of weak Lewis acid. The strong Bronsted acidity, however, was necessary for the isomerization side reactions when using 2-butene or 1-butene as the single reactant in order to produce propylene from the cross metathesis of 1-butene and 2-butene. The results provide easy selection of feedstocks for propylene production when there is olefins price fluctuation.

Acknowledgements

References

1 J. S. Plotkin, The Propylene Quandary, https://www.acs.org/content/acs/en/pressroom/cutting-edge-chemistry/the-propylene-quandary.html, accessed August 8, 2016.

2 K. J. Ivin and J. C. Mol, *Olefin Metathesis and Metathesis Polymerization*, Academic Press, London, 1997.

3 J. C. Mol, *Catal. Today*, 1999, **51**, 289–299.

4 J. C. Mol, *J. Mol. Catal. A: Chem.*, 2004, **213**, 39–45.

5 M. Sibeijn and J. C. Mol, *Appl. Catal.*, 1990, **67**, 279–295.

6 J. A. Moulijn and J. C. Mol, *J. Mol. Catal.*, 1988, **46**, 1–14.

7 A. Andreini, X. Xiaoding and J. C. Mol, *Appl. Catal.*, 1986, **27**, 31–40.

8 M. A. Vuurman, D. J. Stufkens, A. Oskam and I. E. Wachs, *J. Mol. Catal.*, 1992, **76**, 263–285.

9 S. Lwin, C. Keturakis, J. Handzlik, P. Sautet, Y. Li, A. I. Frenkel and I. E. Wachs, *ACS Catal.*, 2015, **5**, 1432–1444.

10 M. A. Vuurman and I. E. Wachs, *J. Phys. Chem.*, 1992, **96**, 5008–5016.

11 S. Vorakitkanvasin, S. K. N. Ayudhya, K. Suriye, P. Praserthdam and J. Panpranot, *Appl. Catal., A*, 2016, **517**, 39–46.

12 S. Lwin, Y. Li, A. I. Frenkel and I. E. Wachs, *ACS Catal.*, 2015, **5**, 6807–6814.

13 S. Lwin and I. E. Wachs, *ACS Catal.*, 2016, **6**, 272–278.

14 B. C. Vicente, R. C. Nelson, A. W. Moses, S. Chattopadhyay and S. L. Scott, *J. Phys. Chem. C*, 2011, **115**, 9012–9024.

15 X. Xiaoding, J. C. Mol and C. Boelhouwer, *J. Chem. Soc., Faraday Trans. 1*, 1986, **82**, 2707–2718.

16 P. Amigues, Y. Chauvin, D. Commereuc, C. T. Hong, C. C. Lai and Y. H. Liu, *J. Mol. Catal.*, 1991, **65**, 39–50.

17 K. Bouchmella, P. Hubert Mutin, M. Stoyanova, C. Poleunis, P. Eloy, U. Rodemerck, E. M. Gaigneaux and D. P. Debecker, *J. Catal.*, 2013, **301**, 233–241.

18 P. Hodges, Propylene price collapse highlights New Normal world, http://www.icis.com/blogs/chemicals-and-the-economy/2016/03/propylene-price-collapse-highlights-new-normal-world/, accessed 9 March, 2016.

19 W. W. Rudolph, R. Mason and C. C. Pye, *Phys. Chem. Chem. Phys.*, 2000, **2**, 5030–5040.

20 I. F. Myronyuk, V. I. Mandzyuk, V. M. Sachko and V. M. Gun'ko, *Nanoscale Res. Lett.*, 2016, **11**, 153.

21 F. Schekler-Nahama, O. Clause, D. Commereuc and J. Saussey, *Appl. Catal., A*, 1998, **167**, 237–245.

22 G. Busca, G. Martra and A. Zecchina, *Catal. Today*, 2000, **56**, 361–370.

23 H. Hu, S. Cai, H. Li, L. Huang, L. Shi and D. Zhang, *J. Phys. Chem. C*, 2015, **119**, 22924–22933.

24 J. G. Amores, V. S. Escribano, G. Ramis and G. Busca, *Appl. Catal., B*, 1997, **13**, 45–58.

25 X. Wang, W. Wu, Z. Chen and R. Wang, *Sci. Rep.*, 2015, **5**, 9766.

26 S. Lwin and I. E. Wachs, *ACS Catal.*, 2014, **4**, 2505–2520.

27 W. Phongsawat, B. Netiworaruksa, K. Suriye, P. Praserthdam and J. Panpranot, *Catal. Lett.*, 2012, **142**, 1141–1149.

28 W. Phongsawat, B. Netiworaruksa, K. Suriye, P. Praserthdam and J. Panpranot, *J. Ind. Eng. Chem.*, 2014, **20**, 145–152.